

## The effect of external control fields on tearing mode dynamics

L. Frassinetti, S. Menmuir, M. W. M. Khan, K. E. J. Olofsson, P. R. Brunsell, J. R. Drake

*Division of Fusion Plasma Physics, Association EURATOM-VR,*

*School of Electrical Engineering, Royal Institute of Technology KTH, SE-10044 Stockholm, Sweden*

### 1. INTRODUCTION

External magnetic perturbations are ubiquitous in magnetic confinement devices. The perturbations can be unavoidable field errors or controlled active perturbations produced by external coil systems. Externally induced magnetic perturbations are used for the suppression of edge localized modes (ELMs) [1] and for the rotation of neoclassical tearing mode islands to positions where the ECCD stabilization is optimal [2]. But the magnetic perturbations also have negative effects on the plasma performances, such as the flow braking. The braking is due to the interaction of a rotating tearing mode with the corresponding static external perturbation and/or to neoclassical toroidal viscosity effects generated by non-resonant external side-band harmonics [3].

This work studies the effect of external resonant magnetic perturbations (RMPs) on the plasma flow and on the tearing mode (TM) dynamics in EXTRAP T2R. EXTRAP T2R is a reversed field pinch equipped with a feedback system that allows the suppression of the entire error field spectrum and the simultaneous generation of clean external perturbations [4,5]. The work describes the RMP effect on the TM velocity on a slow time scale ( $\approx 10\text{ms}$ ) and on a fast time scale ( $\approx 0.1\text{ms}$ ). Then, the TM velocity braking, along with the torque balance equation [6], is used to estimate the plasma viscosity profile.

### 2. RMP EFFECT ON TM VELOCITY ON A SLOW TIME SCALE

In figure 1, the effect of a RMP with harmonic  $(m,n)=(1,-12)$  on the TM velocity and on plasma flow is shown. This harmonic corresponds to the innermost resonant TM in EXTRAP T2R. In figure 1(a), the time evolution of the radial component of the external magnetic

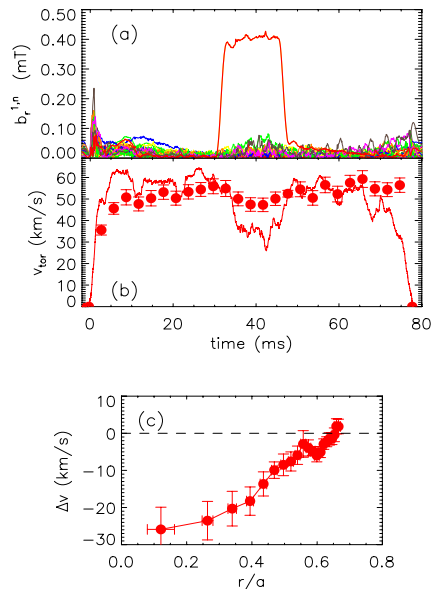


Figure 1. RMP effect on plasma flow and TM velocity. Time evolution of (a) amplitude of the external harmonics and (b) TM toroidal velocity (continuous line) and toroidal flow of OV impurity. The ride lines correspond to the harmonic  $m=1$ ,  $n=-12$  (resonant in the plasma core). Frame (c) shows the profile of the TM velocity variation.

perturbation is shown. An RMP with harmonic (1,-12) and amplitude 0.4mT is applied between 30ms and 45ms. In figure 1(b), the time evolution of the (1,-12) TM toroidal velocity is shown. To highlight the slow time evolution, the signal is smoothed in a 1ms time window. As soon as the RMP is applied, the TM decelerates from  $\approx 55$ km/s to  $\approx 30$ km/s. The red dots in the same figure show the velocity of the OV impurity. In EXTRAP T2R, OV is mainly concentrated in the plasma core and is therefore representative of the core plasma flow (assuming that impurities and plasma co-rotate). The impurity velocity is calculate from the Doppler shift of the OV line intensity measured with a Czerny-Turner spectrometer and is a line integrated measurement. This probably explains the difference in the velocity deceleration between the TM and the flow.

The profile of the TM velocity deceleration is shown in figure 1(c). The deceleration is calculated as the difference of TM velocity during the RMP phase (when the velocity has reached a steady state) and before the RMP phase. Then, the TM deceleration for every mode is plotted at the corresponding resonant radius  $r_s$ . The uncertainty in  $r_s$  is estimated from the variation of the equilibrium parameters during the discharge.

The effect of the RMP amplitude is shown in figure 2. Red dots correspond to the result obtained applying a RMP with harmonic  $n=-12$  and blue dots with harmonic  $n=-15$ . Each dot corresponds to a different shot. All the shots have the same experimental conditions ( $I_p \approx 85$ kA,  $F \approx -0.25$ ) excluding the RMP amplitude. From figure 2(a), it is evident that the increase of the RMP amplitude produces the increase of the velocity braking. In figures 2(b), 2(c) and 2(d), the differences during and before the RMP of plasma current, reversal parameter and intensity of molybdenum impurity are shown, respectively. For RMP amplitudes lower than  $\approx 0.4$ mT, no significant changes in the current, equilibrium and molybdenum impurity content are observed and therefore, the change in the TM velocity can be ascribed only to the increase in the RMP amplitude. For higher RMP amplitudes, it is not possible to exclude that the velocity reduction is influenced also by the

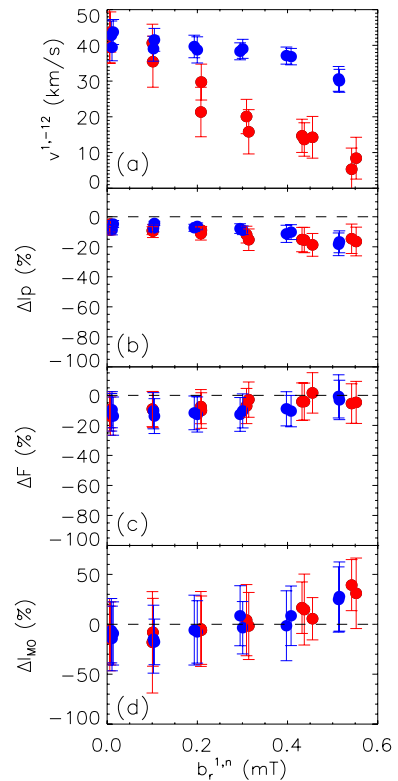


Figure 2. Effects of RMPs with different amplitudes on variation of TM velocity (a), plasma current (b), reversal parameter (c) and molybdenum impurities (d). The red dots corresponds to the effect of a RMP with harmonic  $n=-12$ . The blue dots with harmonic  $n=-15$ .

increase of

impurities and/or by the change in the current. Note from figure 2(a) that a RMP with the same amplitude but with a different harmonic produces a different deceleration. This is shown more in detail in figure 3, where the variation of TM velocity (a), plasma current (b), reversal parameter (c) and molybdenum intensity (d) are shown. All the shots used have the same experimental conditions and a RMP applied from 30ms to 45ms with amplitude 0.4mT, but with a different RMP harmonic (from  $n=-12$  to  $n=-15$ ). The change of the harmonic does not affect the variation of plasma current, reversal and molybdenum. But the effect on the TM velocity is evident. The RMPs with a harmonic resonant closer to the plasma core produce a stronger TM deceleration.

The radial profile of the velocity braking is shown in figure 3(e). The red lines correspond to the effect produced by the RMP with harmonic  $n=-12$ . The maximum velocity variation occurs in the core, where the harmonic  $n=-12$  is resonant. The blue lines correspond to the effect produced by the RMP with harmonic  $n=-15$ . The maximum velocity variation occurs at  $r/a \approx 0.4$ , where the harmonic  $n=-15$  is resonant. This behaviour is consistent with the idea that the plasma flow braking is generated by the interaction of the static RMP with the corresponding rotating TM. Then, the TM velocity deceleration spreads from the resonant radius to the rest of the plasma via the viscous torque effect [6,7].

### 3. RMP EFFECT ON TM VELOCITY ON A FAST TIME SCALE

Figure 1(b) shows the slow TM velocity time evolution before and during the RMP. After a deceleration phase the TM velocity becomes approximately constant. Actually, this steady state is characterized by phases of acceleration followed by phases of deceleration, while only the time averaged velocity is constant. This is shown in figure 4(a) where the velocity profile during a time interval with a RMP of harmonic  $n=-15$  is shown. At the  $n=-15$  resonant radius ( $r/a \approx 0.4$ ) the profile is characterized by evident increases and reductions. The corresponding

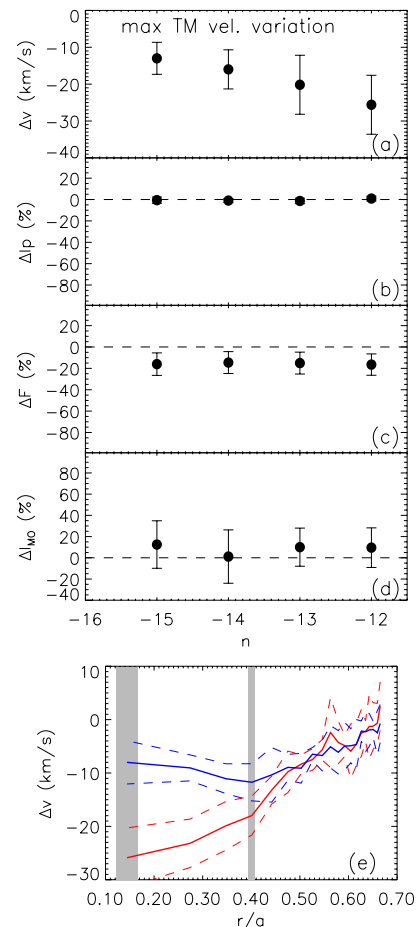


Figure 3. Effect of the RMP harmonic on the TM velocity variation (a),  $I_p$  (b),  $F$  (c) and molybdenum impurities (d). Frame (e) shows the velocity variation profiles for the RMP with harmonic  $n=-12$  (red) and  $n=-15$  (blue). The shaded areas corresponds to the regions were the harmonics  $n=-12$  and  $n=-15$  are resonant.

radial profile time evolution of the velocity variation is shown in figure 4(b). The velocity variation is clearly localized at the  $n=15$  resonance (the dashed line). Then, from this position the velocity perturbation propagates to the core and to the edge.

#### 4. PLASMA VISCOSITY ESTIMATION

From a quantitative point of view, the plasma braking is related to the amplitude of the external perturbation and to plasma characteristics such as the viscosity. The viscosity  $\nu(r)$  can be estimated from the torque balance equation, in which the temporal change in the flow variation profile  $\Delta\Omega(r)$  is related to the electromagnetic torque  $T_{EM}$ , which slows down the flow by acting on the TM velocity, and the viscous torque, which tends to re-establish the unperturbed velocity [6,7]:

$$\rho \frac{\partial \Delta\Omega}{\partial t} = \frac{1}{r} \frac{\partial}{\partial r} \left( r\nu \frac{\partial \Delta\Omega}{\partial r} \right) + \frac{T_{EM}}{4\pi R^3 r} \delta(r - r_s)$$

where  $\rho$  is the plasma density and  $R$  the major radius. To estimate the viscosity, a profile  $\nu(r) = \nu_0(1+cr^\alpha)$  is assumed. The free parameters are calculated in order to obtain the best fit between simulated and experimental velocity variation profiles, as shown in figure 5(a). Errors are estimated by repeating the best fit changing the equilibrium and the density within the experimental uncertainties. The viscosity profile along with the classical viscosity  $\nu = \rho r_i^2 / \tau_i$  (with  $r_i$  the ion gyroradius and  $\tau_i$  the ion collision time) are plotted in figure 5(b).

The viscosity is  $\approx 10^{-7}$  kg/(m·s) and is anomalous, being one order of magnitude larger than the classical viscosity.

#### References

- [1] Evans T.E. *et al.*, Phys. Rev. Lett. 92, 235003 (2004)
- [2] La Haye R.J. *et al.*, Phys. Plasmas 13, 055501 (2006)
- [3] Sun Y. *et al.*, Plasma Phys. Control. Fusion 52, 105007 (2010)
- [4] Olofsson K.E.J. *et al.*, Plasma Phys. Control. Fusion 52, 104005 (2010)
- [5] Frassinetti L. *et al.*, Nucl. Fus. 51, 063018 (2011).
- [6] Fitzpatrick R. and Yu E.P., Phys. Plasmas 6, 3536 (1999)
- [7] Frassinetti L. *et al.*, Nucl. Fus. 50, 035005 (2010).

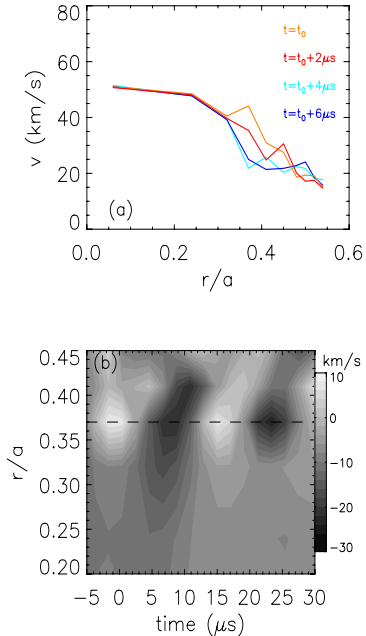


Figure 4. (a) TM velocity profile with a RMP of harmonic  $n=15$  applied. (b) Corresponding radial profile time evolution of the velocity variation.

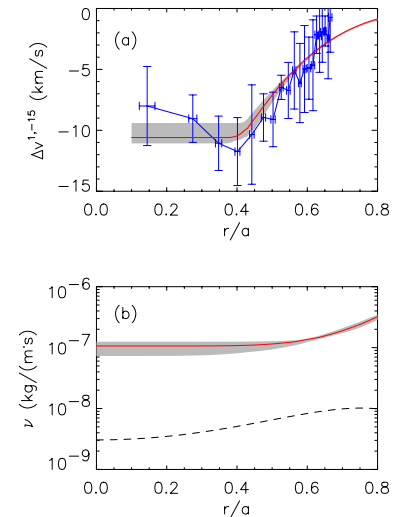


Figure 5. (a) Experimental velocity variation profile (blue) with RMP  $n=15$  and amplitude  $0.4\text{mT}$ . The simulated profile is plotted in red. (b) Corresponding viscosity profile (red line) and classical viscosity (dashed line). Shaded areas highlight the uncertainties.